

# Two Transitions in the Damping of a Unitary Fermi Gas

J. Kinast, A. Turlapov, and J. E. Thomas\*

*Duke University, Department of Physics, Durham, North Carolina, 27708, USA*

(Dated: June 26, 2018)

We measure the temperature dependence of the radial breathing mode in an optically trapped, strongly-interacting Fermi gas of  ${}^6\text{Li}$ , just above the center of a broad Feshbach resonance. The frequency remains close to the unitary hydrodynamic value, while the damping rate reveals transitions at two well-separated temperatures, consistent with the existence of atom pairs above a superfluid transition.

Optically-trapped, unitary Fermi gases [1, 2] test predictions for exotic systems, from nuclear matter [3, 4, 5] and quark-gluon plasmas [6] to high temperature superconductors [7]. Recent measurements of the heat capacity of a unitary gas reveal a transition [8, 9]. This has been interpreted as the onset of superfluidity, using a Bardeen-Cooper-Schrieffer (BCS) – Bose-Einstein Condensate (BEC) crossover approach which was initially developed for high-temperature superconductors [9, 10]. In a unitary Fermi gas, pair interactions between particles are “strong” in the sense that the zero-energy scattering length is much greater than the interparticle spacing, as achieved by tuning near a Feshbach resonance [1]. Such a gas exhibits universal features [1, 3, 11]. At sufficiently low temperatures, unitary Fermi gases are believed to comprise normal atoms, condensed pairs and noncondensed pairs [9, 10]. Fermionic atom pairs are probed in recent projection experiments [12, 13, 14] and in measurements of the pairing gap [15, 16]. Evidence for superfluid hydrodynamics in a unitary gas appears in anisotropic expansion [1] and in the breathing mode frequencies and damping rates [17, 18, 19].

In this Letter, we report the precision measurement of the temperature dependence of the frequency and damping rate for the radial breathing mode of a unitary Fermi gas of  ${}^6\text{Li}$ . We identify two transitions in the damping rate which occur at well-separated temperatures. This is consistent with a qualitative picture of a unitary gas in which the superfluid transition temperature lies well below the temperature at which noncondensed pairs first form [9, 10]. Remarkably, neither transition is accompanied by an abrupt change of the frequency, which in the whole range of temperatures remains within a few percent of the unitary hydrodynamic value. Below the lower transition temperature, the damping rate extrapolates to zero at zero temperature, as expected for a superfluid. The higher temperature transition can be interpreted as arising from the breaking of noncondensed atom pairs by the collective excitation.

In the experiments, we prepare a degenerate 50-50 mixture of the two lowest spin states of  ${}^6\text{Li}$  atoms by forced evaporation [1] in an ultrastable  $\text{CO}_2$  laser trap [20]. At a bias magnetic field  $B$  of 840 G, just above the center of the Feshbach resonance [21, 22], the trap depth is lowered by a factor of  $\simeq 580$  in a few seconds [1, 17] and

then recompressed to 4.6% (for most of the experiments) of the full trap depth in 1.0 s and held for 0.5 s to assure equilibrium. A controlled amount of energy is added to the gas by releasing the atoms from the trap for a short time and then recapturing the cloud [8, 9]. The gas is then allowed to thermalize for 0.1 s.

The radial breathing mode is excited by releasing the cloud and recapturing the atoms after  $25\ \mu\text{s}$  (for 4.6% trap depth). After the excitation, we let the cloud oscillate for a variable time  $t_{\text{hold}}$ , at the end of which the gas is released and imaged after  $\simeq 1$  ms of expansion [1, 9, 17].

Radial breathing mode frequencies  $\omega$  and damping times  $\tau$  are determined from the oscillatory dependence of the released cloud size on  $t_{\text{hold}}$  [17, 18, 19]. For each temperature, 60-90 values of  $t_{\text{hold}}$  are chosen in the time range of interest. These values of  $t_{\text{hold}}$  are randomly ordered during data acquisition to avoid systematic error. Three full sequences are obtained and averaged. The averaged data is fit with a damped sinusoid  $x_0 + A \exp(-t/\tau) \sin(\omega t + \varphi)$ . We have obtained oscillation curves at 30 different temperatures, containing data from 6300 repetitions of the experiment.

For most of the data reported, the total number of atoms is  $N = 2.0(0.2) \times 10^5$ . From the measured trap frequencies, corrected for anharmonicity, we obtain for 4.6% trap depth:  $\omega_{\perp} = \sqrt{\omega_x \omega_y} = 2\pi \times 1696(10)$  Hz,  $\omega_x/\omega_y = 1.107(0.004)$ , and  $\omega_z = 2\pi \times 71(3)$  Hz, so that  $\bar{\omega} = (\omega_x \omega_y \omega_z)^{1/3} = 2\pi \times 589(5)$  Hz is the mean oscillation frequency and  $\lambda = \omega_z/\omega_{\perp} = 0.045$  is the anisotropy parameter. The typical Fermi temperature  $T_F = (3N)^{1/3} \hbar \bar{\omega} / k_B$  of a corresponding noninteracting gas is  $\simeq 2.4\ \mu\text{K}$ , small compared to the final trap depth of  $U_0/k_B = 35\ \mu\text{K}$  (at 4.6% of full depth). The coupling parameter of the strongly-interacting gas at  $B = 840$  G is  $k_F a \simeq -30.0$ , where  $\hbar k_F = \sqrt{2m k_B T_F}$  is the Fermi momentum, and  $a = a(B)$  is the zero-energy scattering length estimated from Ref. [21].

The dimensionless empirical temperature  $\tilde{T}$  is determined by the method implemented in [8, 9]: The column density of the cloud is spatially integrated in the axial direction to yield a normalized (integrates to 1), one dimensional, transverse spatial distribution  $n(x)$ . This distribution is fit to determine the empirical reduced temperature  $\tilde{T}$  using a finite temperature Thomas-Fermi profile with a fixed Fermi radius, which is measured in a sepa-

rate experiment at the lowest temperatures [8, 9]. The empirical temperature  $\tilde{T}$  is numerically calibrated to the theoretical reduced temperature  $T/T_F$  [9, 10]. In Ref. [9], we show that a simple approximation relating  $\tilde{T}$  to  $T/T_F$  is given by,

$$\tilde{T} \simeq \tilde{T}_{nat} \equiv \frac{T}{T_F \sqrt{1 + \beta}}. \quad (1)$$

Eq. 1 yields accurate values of  $T/T_F$  for  $\tilde{T} \geq 0.45$  and provides a reasonable estimate at lower temperatures, where higher precision can be obtained using the calibration [9]. Here  $\beta$  is the unitary gas parameter [1, 3, 5, 23, 24], which we recently measured to be  $\beta = -0.49(0.04)$  (statistical error only) [8, 9].

The mode frequency provides important information on the state of the system. The frequency versus the empirical temperature for experiments at 4.6% trap depth is shown in Fig. 1. The figure shows the measured frequen-

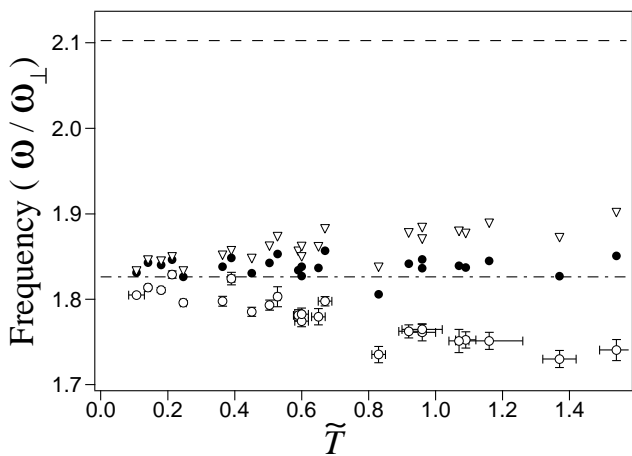


FIG. 1: Frequency  $\omega$  versus empirical reduced temperature  $\tilde{T}$ : Raw data (empty circles with error bars); Data corrected for anharmonicity: Black dots— using a zero-temperature Thomas-Fermi profile and Triangles— using a finite-temperature Thomas-Fermi profile. The dot-dashed line is the unitary hydrodynamic frequency  $\omega_H = \sqrt{10/3}\omega_\perp$ . The dashed line at the top of the scale is the frequency  $2\omega_x$  observed for a noninteracting gas at the lowest temperatures.

cies  $\omega_{\text{meas}}$  (open circles), uncorrected for anharmonicity in the trapping potential, as well as the frequencies after correction by two different methods. The frequency correction is proportional to the ratio  $\langle \rho^4 \rangle / \langle \rho^2 \rangle$  [25], where  $\rho$  is the transverse radius of the expanded cloud. For an isentropic unitary gas, we obtain [26]

$$\omega = \omega_{\text{meas}} \left( 1 + \frac{2}{5} \frac{m\omega_\perp^2}{U_0} \frac{\langle \rho^4 \rangle}{\langle \rho^2 \rangle b_H^2} \right), \quad (2)$$

with  $b_H$  a hydrodynamic scale factor [1, 27]. For 1 ms of expansion, we obtain  $b_H = 13.3$ .

The first method for estimating  $\langle \rho^4 \rangle / \langle \rho^2 \rangle$  assumes that the spatial distribution of the gas is nearly a zero-temperature Thomas-Fermi profile, which is a good approximation at the lowest temperatures. In this case, the corrected frequency is [25, 26]

$$\omega = \omega_{\text{meas}} \left( 1 + \frac{32}{25} \frac{m\omega_\perp^2}{U_0} \frac{\langle x^2 \rangle}{b_H^2} \right), \quad (3)$$

where  $\langle x^2 \rangle$  is the transverse mean square width of the gas in the x-direction after the expansion. Applying this method over the whole temperature range, we find that the corrected frequencies (black dots in Fig. 1) remain very close to the unitary, hydrodynamic value, shown as a dot-dashed line.

In the second method, we include the effects of the finite temperature on the spatial profile of the cloud by calculating the ratio  $\langle \rho^4 \rangle / \langle \rho^2 \rangle = (4/3) \langle x^4 \rangle / \langle x^2 \rangle$  directly from the fitted one-dimensional finite temperature Thomas-Fermi profiles. The corrected frequencies are displayed in Fig. 1 as open triangles. The higher order corrections have been calculated and are found to be negligible.

The radial breathing frequency varies smoothly over the whole temperature range, and remains close to the value  $\omega_H = \sqrt{10/3}\omega_\perp = 1.83\omega_\perp$  predicted by hydrodynamic theory for a unitary gas, where  $1/(k_F a) = 0$  [28, 29, 30, 31, 32, 33]. Such temperature independence has been observed previously in a BEC [34]. For the unitary Fermi gas, the observed frequencies are far from  $2\omega_x = 2.10\omega_\perp$ , the value observed for a noninteracting gas at the lowest temperatures, which is shown as a dashed line at the top of Fig. 1. This, as well as the observed hydrodynamic expansion, justifies the use of the hydrodynamic expansion factor  $b_H$  in Eqs. 2 and 3 over the whole temperature range.

The frequencies obtained using the finite temperature corrections (triangles in Fig. 1) rise 4% above  $\omega_H$  at the highest temperatures. This can be explained by the slow decrease in the collision rate of the unitary gas at higher temperatures [35], which makes the gas slightly less hydrodynamic and pulls the frequency up toward the noninteracting gas value. The slow increase in frequency is consistent with our previous estimate of the reduced temperature for ballistic expansion of the unitary gas,  $T/T_F \geq 3$  [1, 35].

In contrast to the frequency, the damping rate of the radial breathing mode reveals two transitions, at  $\tilde{T} \simeq 0.5$  and at  $\tilde{T} \simeq 1.0$ , as shown in Fig. 2.

The lower transition at  $\tilde{T} = 0.5$  is indicative of a superfluid phase transition, consistent with our previous study of damping versus temperature [17]. Between  $\tilde{T} = 0.1$  and  $\tilde{T} = 0.5$ , the damping rate decreases with decreasing  $\tilde{T}$ , the opposite of the behavior expected for a degenerate, collisionally hydrodynamic gas [36, 37, 38] and consistent with a superfluid picture [17]. This behavior is

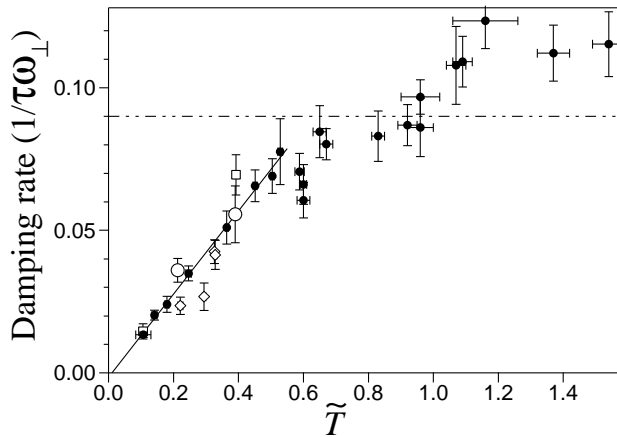


FIG. 2: Temperature dependence of the damping rate for the radial breathing mode of a trapped  ${}^6\text{Li}$  gas at 840 G, showing two transitions. Solid dots are the main data set taken at 4.6% trap depth. Other symbols are for the system with scaled parameters: Two squares – at 0.85% of full trap depth; Four diamonds – at 19% of full trap depth; Two open circles – at 3 times smaller number of atoms. The dot-dashed line is the maximum damping rate for a classical harmonically trapped gas with binary collisions. The solid line is Eq. (4) which extrapolates close to zero at zero temperature.

similar to that observed in the radial breathing mode of a BEC [34]. For  $0.65 \leq \tilde{T} \leq 1.0$ , the damping rate is nearly independent of temperature. This change in behavior is accompanied by a significant, reproducible notch in the damping rate near  $\tilde{T} = 0.6$ . Using Eq. 1, we find that  $\tilde{T} = 0.5$  corresponds to  $T/T_F = 0.35$ . This transition temperature is somewhat higher than the predicted superfluid transition temperature of  $T_c = 0.29 T_F$ , as well as the value  $T_c = 0.27 T_F$  estimated from the observed slope change in the heat capacity, after temperature calibration [9]. However, it is not clear that the observed change in the damping rate should occur precisely at the same temperature as for the change in heat capacity [9].

Damping below  $\tilde{T} = 0.5$  may arise from the interaction between a superfluid core and a normal gas in the edges of the cloud. Normal fermionic excitations are present even when the core is superfluid [39], because the local Fermi energy at the edges can be smaller than  $k_B T_c$ . It is possible that the transition near  $\tilde{T} = 0.5$  arises as the core of the cloud changes from superfluid to collisional as the temperature increases. Indeed, in the temperature region from  $0.65 \leq \tilde{T} \leq 1.0$ , the damping rate is close to the maximum allowed for a collisional gas  $1/\tau = 0.09 \omega_\perp$  [37].

The higher temperature transition region,  $1.0 \leq \tilde{T} \leq 1.2$ , may arise from the breaking of noncondensed pairs. In this region, the frequency remains near the unitary hydrodynamic value while the damping rate rises roughly linearly with increasing  $\tilde{T}$  from approximately the maximum value allowed for a collisional gas,  $1/\tau = 0.09 \omega_\perp$  [37], to a value roughly 1.5 times larger, signal-

ing the appearance of a new channel of energy loss. The temperature range over which this transition occurs is much smaller than the temperature scale, of order  $T_F$ , over which the binary collision rate of a unitary gas decreases in this temperature region [35]. Although the frequency is nearly constant, this increase in damping rate resembles that which we observed at low temperature, at a magnetic field of 1080 G, where the coupling is reduced to  $k_F a = -1.35$  [19]. Similar behavior was first observed in Ref. [18] and attributed to a pair breaking process [18, 19]. The enhanced damping in all of these experiments may be of the same nature: both the decrease in coupling and the increase in temperature reduce the pairing gap, making it comparable to the collective excitation energy  $\hbar\omega$  and therefore, causing fermion pairs to break.

The second transition region occurs at high temperatures where the energy of a strongly-interacting Fermi gas merges with that of an ideal noninteracting Fermi gas [8, 9, 10]. Using Eq. 1, we see that the second transition region  $1.0 \leq \tilde{T} \leq 1.2$ , corresponds to  $0.71 \leq T/T_F \leq 0.86$ , close to the temperature range estimated for the vanishing of noncondensed pairs [9, 10, 40]. In principle, merging of the ideal and unitary gas energies near  $T_F$  can arise (at least in part) because the unitary gas becomes classical at high temperatures. However, the appearance of enhanced damping supports the concept that the binding energy of noncondensed pairs is decreasing as part of the merging process [9, 10], causing collective excitations to break pairs.

We have investigated the possibility that the observed variation of the damping rate with temperature might arise in part from oscillations of different components of the gas at different frequencies. In a Bose-Einstein condensate with a thermal cloud, such behavior leads to revivals of the net oscillation amplitude, altering the apparent decay rates [41]. In the present experiments, we find no evidence for such revivals, even after increasing the time over which the decay of the mode is observed.

The near linear dependence of the damping rate on  $\tilde{T}$  in the region  $0.1 \leq \tilde{T} \leq 0.5$  is well fit by

$$\frac{1}{\tau \omega_\perp} = 0.146 (0.004) \tilde{T} - 0.0015 (0.0014), \quad (4)$$

for the main data set taken at 4.6% trap depth and  $N = 2 \times 10^5$  atoms. The damping rate extrapolates close to zero at zero temperature, consistent with a superfluid.

We have examined the dependence of the damping rate on the trap oscillation frequency  $\omega_\perp$  and on the number of atoms  $N$ . Dimensional analysis requires that  $1/\tau = \omega_\perp f(T/T_F, N, \lambda)$ , where  $f$  is a dimensionless function.

For fixed  $T/T_F$  (or fixed  $\tilde{T}$ ), we find that the function  $f$  cannot have a strong number dependence. For example, it cannot be  $\propto k_B T_F / (\hbar \omega_\perp) \propto N^{1/3}$  or its inverse. This is established by examining the scaling of the damping rate with the atom number. We find that the damping

rate at 4.6% of full trap depth does not change appreciably when the number is reduced by a factor of  $\simeq 3$ : The damping rate at reduced number, open circles in Fig. 2, lies very close to the main data set (solid dots) when plotted versus  $\tilde{T}$ . Hence, it is likely that  $1/\tau$  depends on  $N$  only via the combination  $T/T_F$ , and the most general formula for  $1/\tau$  is then limited to

$$\frac{1}{\tau} = \omega_{\perp} f\left(\frac{T}{T_F}, \lambda\right). \quad (5)$$

Experimentally, we are not able to test whether the damping rate depends on  $\lambda$ . We have verified that  $1/\tau$  versus  $\tilde{T}$  scales approximately as  $\omega_{\perp}$  by monitoring the breathing mode in the trap at 0.85% of full depth ( $\omega_{\perp} = 728(4)$  Hz, squares in Fig. 2) and at 19% ( $\omega_{\perp} = 3343(20)$  Hz, diamonds). In both cases,  $1/\tau$  in units of  $\omega_{\perp}$  is comparable to that of the main data set.

Quantum viscosity [42] recently has been suggested as the mechanism for the small damping rate observed for the axial breathing mode in Ref. [18]. The quantum viscosity  $\eta$  is of order  $\hbar k_F/\sigma$ , where the collision cross section  $\sigma \propto 1/k_F^2$  in the unitary limit [1]. Hence,  $\eta \propto \hbar k_F^3 \propto \hbar n$ , where  $n$  is the density. For our system, the radial damping rate arising from quantum viscosity is estimated to be  $1/(\tau\omega_{\perp}) = 3 \times 10^{-5}$ . This is consistent with the extrapolated value at  $T = 0$ , but cannot explain the observed rates of order  $0.014\omega_{\perp}$  at our lowest temperature. Hence, the decay of the radial mode is probably by a different mechanism.

This research is supported by the Physics Divisions of the Army Research Office and the National Science Foundation, the Chemical Sciences, Geosciences and Biosciences Division of the Office of Basic Energy Sciences, Office of Science, U. S. Department of Energy, and the Fundamental Physics in Microgravity Research program of the National Aeronautics and Space Administration.

---

\* jet@phy.duke.edu

- [1] K. M. O'Hara, S. L. Hemmer, M. E. Gehm, S. R. Granade, and J. E. Thomas, *Science* **298**, 2179 (2002).
- [2] J. E. Thomas and M. E. Gehm, *Am. Scientist* **92**, 238 (2004).
- [3] H. Heiselberg, *Phys. Rev. A* **63**, 043606 (2001).
- [4] G. A. Baker, Jr., *Phys. Rev. C* **60**, 054311 (1999).
- [5] J. Carlson, S.-Y. Chang, V. R. Pandharipande, and K. E. Schmidt, *Phys. Rev. Lett.* **91**, 050401 (2003).
- [6] P. F. Kolb and U. Heinz, *Quark Gluon Plasma 3* (World Scientific, 2003), p. 634, see Hydrodynamic Description of Ultrarelativistic Heavy Ion Collisions, arXiv:nucl-th/0305084.
- [7] Q. Chen, J. Stajic, S. Tan, and K. Levin (2004), arXiv:cond-mat/0404274.
- [8] J. Kinast, A. Turlapov, and J. E. Thomas (2004), arXiv:cond-mat/0409283.
- [9] J. Kinast, A. Turlapov, J. E. Thomas, Q. Chen, J. Stajic, and K. Levin, *Science* **27** January 2005 (10.1126/science.1109220).
- [10] Q. Chen, J. Stajic, and K. Levin (2004), arXiv:cond-mat/0411090.
- [11] T.-L. Ho, *Phys. Rev. Lett.* **92**, 090402 (2004).
- [12] C. A. Regal, M. Greiner, and D. S. Jin, *Phys. Rev. Lett.* **92**, 040403 (2004).
- [13] M. W. Zwierlein, C. A. Stan, C. H. Schunck, S. M. F. Raupach, A. J. Kerman, and W. Ketterle, *Phys. Rev. Lett.* **92**, 120403 (2004).
- [14] M. W. Zwierlein, C. H. Schunck, C. A. Stan, S. M. F. Raupach, and W. Ketterle (2004), arXiv:cond-mat/0412675.
- [15] C. Chin, M. Bartenstein, A. Altmeyer, S. Riedl, S. Jochim, J. H. Denschlag, and R. Grimm, *Science* **305**, 1128 (2004).
- [16] M. Greiner, C. A. Regal, and D. S. Jin (2004), arXiv:cond-mat/0407381.
- [17] J. Kinast, S. L. Hemmer, M. E. Gehm, A. Turlapov, and J. E. Thomas, *Phys. Rev. Lett.* **92**, 150402 (2004).
- [18] M. Bartenstein, A. Altmeyer, S. Riedl, S. Jochim, C. Chin, J. H. Denschlag, and R. Grimm, *Phys. Rev. Lett.* **92**, 203201 (2004).
- [19] J. Kinast, A. Turlapov, and J. E. Thomas, *Phys. Rev. A* **70**, 051401(R) (2004).
- [20] K. M. O'Hara, S. R. Granade, M. E. Gehm, T. A. Savard, S. Bali, C. Freed, and J. E. Thomas, *Phys. Rev. Lett.* **82**, 4204 (1999).
- [21] M. Bartenstein, A. Altmeyer, S. Riedl, R. Geursen, S. Jochim, C. Chin, J. H. Denschlag, R. Grimm, A. Simoni, E. Tiesinga, et al. (2004), arXiv:cond-mat/0408673.
- [22] C. H. Schunck, M. W. Zwierlein, C. A. Stan, S. M. F. Raupach, W. Ketterle, A. Simoni, E. Tiesinga, C. J. Williams, and P. S. Julienne (2004), arXiv:cond-mat/0407373.
- [23] M. E. Gehm, S. L. Hemmer, S. R. Granade, K. M. O'Hara, and J. E. Thomas, *Phys. Rev. A* **68**, 011401(R) (2003).
- [24] A. Perali, P. Pieri, and G. C. Strinati, *Phys. Rev. Lett.* **93**, 100404 (2004).
- [25] This frequency shift was first derived by S. Stringari, private communication.
- [26] We ignore here an additional small correction  $\lambda^2 \langle z^2 \rho^2 \rangle / (4 \langle \rho^2 \rangle)$ . This changes the coefficient in Eq. 2 from  $2/5$  to  $2/5 + 1/16$ . In the zero temperature Thomas-Fermi approximation, Eq. 3, the coefficient changes from  $32/25$  to  $32/25 + 1/5$ . The corresponding coefficient in the noninteracting gas correction [17, 19] is also increased from  $6/5$  to  $7/5$ .
- [27] C. Menotti, P. Pedri, and S. Stringari, *Phys. Rev. Lett.* **89**, 250402 (2002).
- [28] S. Stringari, *Europhys. Lett.* **65**, 749 (2004).
- [29] H. Heiselberg, *Phys. Rev. Lett.* **93**, 040402 (2004).
- [30] H. Hu, A. Minguzzi, X.-J. Liu, and M. P. Tosi, *Phys. Rev. Lett.* **93**, 190403 (2004).
- [31] Y. E. Kim and A. L. Zubarev, *Phys. Lett. A* **327**, 397 (2004).
- [32] Y. E. Kim and A. L. Zubarev, *Phys. Rev. A* **70**, 033612 (2004).
- [33] N. Manini and L. Salasnich (2004), arXiv:cond-mat/0407039.
- [34] F. Chevy, V. Bretin, P. Rosenbusch, K. W. Madison, and

- J. Dalibard, Phys. Rev. Lett. **88**, 250402 (2002).
- [35] M. E. Gehm, S. L. Hemmer, K. M. O'Hara, and J. E. Thomas, Phys. Rev. A **68**, 011603(R) (2003).
- [36] L. Vichi, J. Low Temp. Phys. **121**, 177 (2000).
- [37] D. Guéry-Odelin, F. Zambelli, J. Dalibard, and S. Stringari, Phys. Rev. A **60**, 4851 (1999).
- [38] P. Massignan, G. M. Bruun, and H. Smith (2004), arXiv:cond-mat/0409660.
- [39] J. Stajic, Q. Chen, and K. Levin, Phys. Rev. Lett. **94**, 060401 (2005).
- [40] The pairing gap has been calculated as a function of temperature, Q. Chen and K. Levin, private communication. Above  $T \simeq 0.75 T_F$ , the trap-averaged gap is less than  $\hbar\omega = 0.06 k_B T_F$ , the breathing mode oscillation energy for the conditions of our trap.
- [41] B. Jackson and C. S. Adams, Phys. Rev. A **63**, 053606 (2001).
- [42] B. A. Gelman, E. V. Shuryak, and I. Zahed (2004), arXiv:nucl-th/0410067.